JOURNAL OF MATERIALS SCIENCE 23 (1988) 161–167

Particle size distribution in rubber modified polyamides 6

L. D'ORAZIO, C. MANCARELLA, E. MARTUSCELLI
Istituto di Ricerche su Tecnologia dei Polimeri e Reologia Via Toiano, 6 – Arco Felice, Napoli, Italy

Particle size and particle-size distribution in rubber-toughened polyamides 6 (PA6) were determined according to the Schwartz–Saltikov method. The quantitative morphological analysis was performed on microtomed samples of binary and ternary blends containing ethylene–propylene random copolymer (EPR) and functionalized EPR rubber (EPR-g-SA). The blends were obtained according to two different methods: concurrent to the hydrolitic polymerization of caprolactam, and simultaneous melt mixing. The formation of an (EPR-g-SA)-g-PA6 copolymer during blending was assumed to occur in the ternary blends. Correlations between particle size, particle size distribution, preparation method, composition and Izod impact strength of such materials were investigated.

1. Introduction

The particle-size distribution of the dispersed phase is one of the most important factors in determining the final properties of incompatible polymer–polymer blends and alloys [1]. Generally the mode and state of dispersion of the minor component depends on the composition, blending procedure and processing. Moreover it has been found that the addition of emulsifier and/or compatibilizing agents may drastically reduce the average dimensions of dispersed particles and induce a stronger adhesion with the matrix [2].

In the present paper we report the results of an accurate and thorough morphological analysis carried out in order to determinate size, size distribution and volumetric fraction of rubbery particles dispersed as toughening agents in polyamides 6. An amorphous ethylene–propylene random copolymer (EPR) and a modified EPR (EPR-g-succinic anhydride (EPR-g-SA) were used as impact modifier of the PA6.

The determination of particle-size distribution and volumetric fraction was performed on samples of blends obtained by two different methods: (a) concurrent with hydrolitic polymerization of ε-caprolactam, and (b) simultaneous melt mixing of the components. The method of EPR modification, blend preparation, morphology and properties of binary PA6/EPR and ternary PA6/EPR/EPR-g-SA were reported in previous works [3–5]. The formation of an EPR-g-SA-PA6 graft copolymer during blending was assumed to occur in the case of blends containing the functionalized EPR-g-SA rubber.

A detailed and thorough investigation of the mode and state of dispersion of the rubbery phase in such materials was undertaken with the aim of studying: (i) the relationships between particle size, particle size distribution, preparation method and composition of the blends; (ii) the influence, in the ternary blends, of the content of functionalized rubber (EPR-g-SA) on the particle size and particle-size distribution; and (iii) the correlations between particle size, particle-size distribution and Izod impact strength of the binary and ternary blends.

2. Theory

Assuming that the dispersed particles closely approach spherical shape, a mathematical procedure was developed for converting the two-dimensional distribution of particle sections into the corresponding three-dimensional distribution of particle size. The number and the size of the circular traces resulting when the particles are intersected by a random plane can be counted and measured by means of SEM. Then the probable number and size of the spheres that give rise to the observed section distribution can be deduced.

If the spheres in the blends all have the same size (monodispersed system) an extremely simple and general equation applies. It relates the number of particle sections observed per unit area (N_A) to the number of spheres per unit volume (N_v)

$$N_v = N_A/D_j \quad (1)$$

where D_j is the diameter of spheres. It should be emphasized that N_A involves the number of particle sections of all sizes per unit area.

When particle sections of only one particular size (d_i) are counted, a probability factor must be introduced to account for the arbitrary restriction imposed. Under these conditions Equation 1 becomes

$$N_v = \frac{N_A(i,j)}{p}\frac{1}{D_j} \quad (2)$$

where p is the probability of the plane intersecting a sphere of diameter D_j so as to yield sections of size d_i and $N_A(i, j)$ is the number of sections of diameter d_i per unit area obtained from spheres of diameter D_j. The probability that a random plane intersects a spherical particle between distances h_i and $h(i-1)$ from the centre giving rise to circular sections with

0022–2461/88 $03.00 + .12

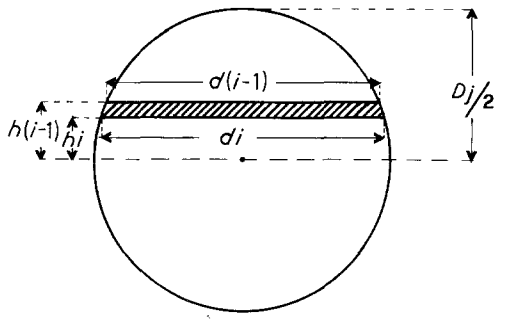

Figure 1 Intersection of a spherical particle by a random plane.

diameters between di and $d(i-1)$ is equal to the thickness h of the circular slice divided by the particle radius. This situation is shown in Fig. 1.

$$p = \frac{h}{D_j/2} = \frac{h(i-1) - h_i}{D_j/2} \quad (3)$$

In the case of a polydispersed system of spherical particles intersected by a random plane, some of the observed sections derive from particles of larger sizes. The number of these latter sections must be subtracted from the total number in order to obtain those sections due only to the particles of one size.

The mathematical procedure developed for converting distribution of section diameters into distribution of particle size was made according to the Schwartz–Saltikov methods [6], breaking down the particle size into 15 groups. The basic equation relating the number of particle sections per unit area to the number of particles per unit volume for particles of one diameter was

$$N_A(i,j) = N_v(j)\Delta\{[j^2 - (i-1)^2]^{1/2} - [(j^2 - i)^2]^{1/2}\} \quad (4)$$

where the first index designates the diameter of the sections, the second one refers to the size of the particles, which form the given sections on the random plane, and Δ is the ratio between the observed maximum particle diameter and the number of the fixed groups.

The mathematical corrections, developed for converting the distribution of visible section diameters into distribution of real size of particles yield a shift of the maximum of frequency distributions towards larger particles.

3. Experimental details

3.1. Materials

The caprolactam (CL) and aminocaproic acid (ACA) used in this work were FLUKA purum products employed without further purification. The polyamide 6 (PA6) used was SNIAMID ASN 27/S produced by SNIA having a number average molecular weight ($\overline{M_n}$) of 2.3×10^4. Before use, the PA6 was kept under vacuum at 60° C for 48 h to eliminate the water content stored during industrial washing. Xylene, Carlo Erba, RPE grade was passed over neutral alumina and collected under nitrogen before use.

The ethylene–propylene random copolymer (EPR) was a Dutral CO/054 supplied by Dutral s.p.a. having a weight-average molecular weight ($\overline{M_w}$) of 1.80×10^5, and an ethylene content (C_2) of 60 mol % and a glass transition temperature (T_g) of −60° C.

The modified EPR, bearing along its backbone 3 wt % by weight succinic anhydride groups (EPR-g-SA) was prepared following the same procedure already described elsewhere [3].

TABLE I Compositions of the investigated blends obtained directly during caprolactam polymerization; the preparation method is indicated

Code	PA6 content (wt %)	EPR content (wt %)	EPR-g-SA content (wt %)	Preparation method
A_1	90	10	0	Solution
A_2	90	10	0	Bulk
B_2	80	20	0	Bulk
C_1	80	18	2	Solution
C_2	80	18	2	Bulk
D_1	80	15	5	Solution
D_2	80	15	5	Bulk

3.2. Blending

3.2.1. Concurrent blending with caprolactam polymerization

Such blends were obtained directly during caprolactam polymerization via a hydrolitic process. Two different methods of blend preparation were followed: the first (solution method) involved a preliminary dispersion of the rubber in xylene. The second (bulk method) was characterized by the fact that the rubber is directly added to caprolactam and initiator and dispersed by mechanical stirring before polymerization. Further details are reported in a previous paper [4]. The examined blend compositions, together with the preparative method, are indicated in Table I.

3.2.2. Blending by melt mixing

All the binary and ternary blends were prepared in a Brabender-like apparatus (Rheocord E.C. of Haake Inc.) by a simultaneous melt-mixing of all the components at a temperature of 260 ± 3° C with a mixing time of 20 min and at a rotation speed of rollers of 32 r.p.m. The examined blend compositions are reported in Table II.

3.3. Specimen preparation and conditioning

The blended materials were compression moulded in a heated press (Wabosh Hydraulic Press) at a temperature of 260 ± 5° C and a pressure of 240 ± 20 kg cm^{-2} into 3 mm thick sheets. The samples so obtained were water conditioned before examining following a procedure elsewhere described [3].

TABLE II Compositions of the investigated blends obtained by one-step melt-mixing

Code	PA6 content (wt %)	EPR content (wt %)	EPR-g-SA content (wt %)
A_3	90	10	0
B_3	80	20	0
D_3	80	15	5
E_3	80	10	10

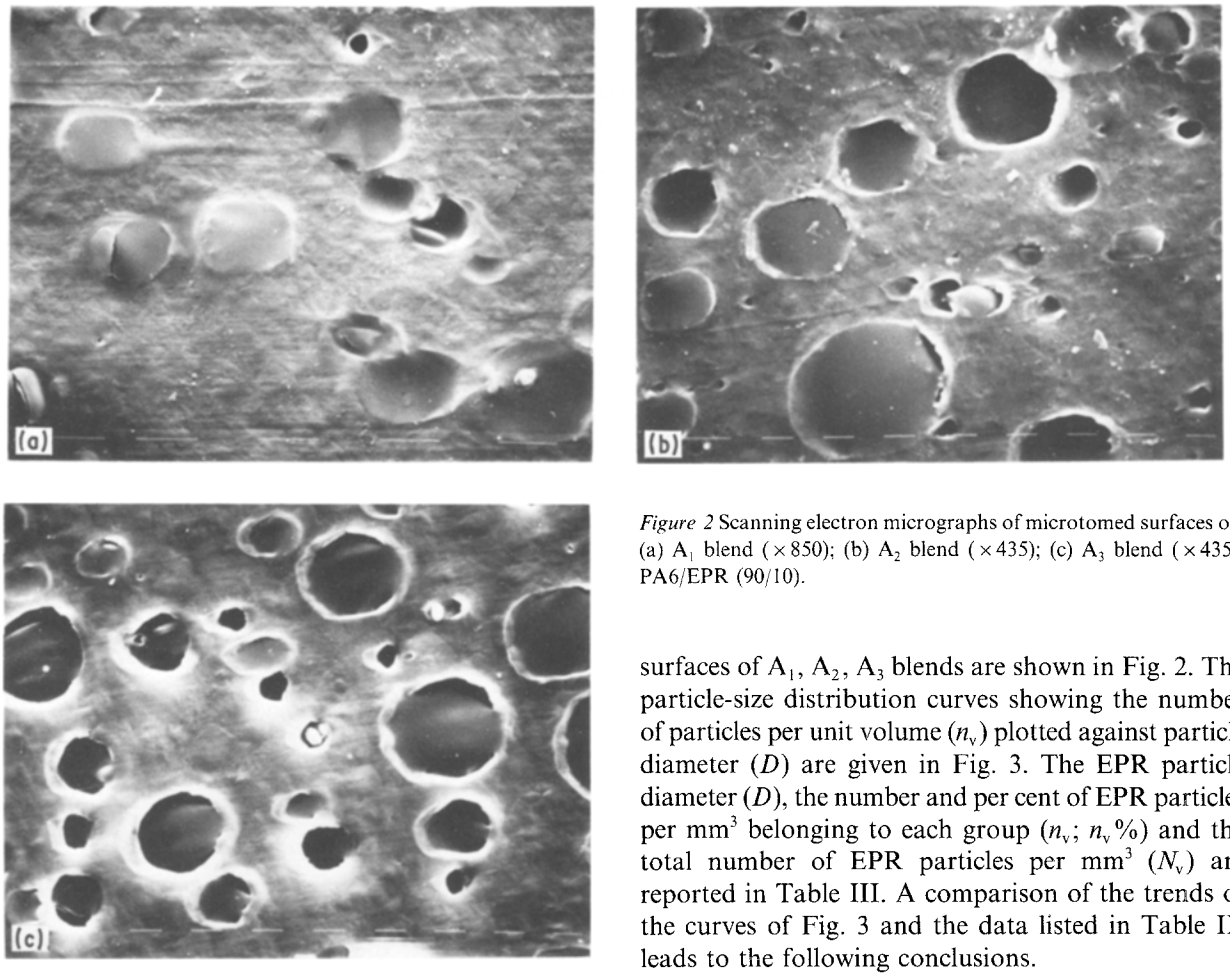

Figure 2 Scanning electron micrographs of microtomed surfaces of: (a) A_1 blend (×850); (b) A_2 blend (×435); (c) A_3 blend (×435). PA6/EPR (90/10).

3.4. Techniques

Samples of binary and ternary blends were faced in an ultramicrotome (LKB Ultratome III) at room temperature. The smooth surfaces were coated with gold–palladium by means of a Polaron sputtering and subsequently analysed using a scanning electron microscope (SEM 501 Philips) at suitable magnification. The diameters of the observed particle sections were manually measured on the scanning electron micrographs using a ruler.

4. Results and discussion

4.1. Particle-size distribution in PA6/EPR binary blends

Typical scanning electron micrographs of microtomed surfaces of A_1, A_2, A_3 blends are shown in Fig. 2. The particle-size distribution curves showing the number of particles per unit volume (n_v) plotted against particle diameter (D) are given in Fig. 3. The EPR particle diameter (D), the number and per cent of EPR particles per mm^3 belonging to each group (n_v; n_v%) and the total number of EPR particles per mm^3 (N_v) are reported in Table III. A comparison of the trends of the curves of Fig. 3 and the data listed in Table III leads to the following conclusions.

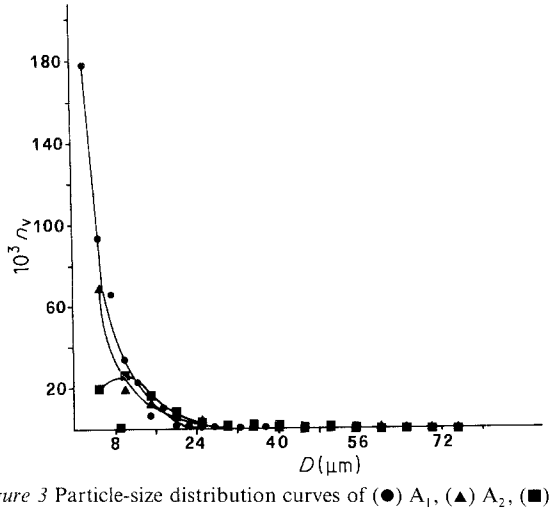

Figure 3 Particle-size distribution curves of (●) A_1, (▲) A_2, (■) A_3 blends.

1. The total number of dispersed EPR particles per unit volume (N_v) is influenced by the blending procedure. The largest value of N_v is observed in the case of A_1 blend. (N_v = 415 877; 111 488 and 74 000 for A_1, A_2 and A_3 blends, respectively.)

2. The particle-size distribution curve of A_1 is characterized by a larger presence of particles having dimensions comparatively smaller than those observed for A_2 and A_3 blends. Moreover, in A_1 blend the dispersion of particle size is narrower than in A_2 and A_3 blends. (Most of the EPR domains exhibit a diameter ranging from 2.5 to 17.5 μm.)

3. Particles with almost the same dimensions are found in A_2 and A_3 blends. Nevertheless, the particle-size distribution curves look different. In the region of lowest diameters it can, in fact, be observed that A_2 blend shows n_v values higher than those of A_3 blend (for D = 5.0, n_v = 68 288 and 19 752 for A_2 and A_3, respectively).

4. The A_3 blend is characterized by the most homogeneous distribution of particle size.

The values of the volumetric fraction of the rubbery phase, estimated from the particle-size distribution are 16.1%, 17.8%, 16.5% for A_1, A_2, A_3 blends, respectively. Such values are in agreement with those calculated on the basis of composition and density of the components (16.6%). Such results strongly support the hysteresis that the particles dispersed do not contain any polyamide inclusions.

The Izod impact behaviour of A_1, A_2 and A_3 blends, has been studied and the results were reported in previous papers [3, 4]. It was found that A_1 blend shows better impact properties than of A_2 and A_3

TABLE III Particle diameters (D), number and per cent particles per volume unit (n_v and n_v %) of A_1, A_2 and A_3 blends. N_v is the total number of particles per volume unit

A_1			A_2			A_3		
D (μm)	n_v	n_v (%)	D (μm)	n_v	n_v (%)	D (μm)	n_v	n_v (%)
2.5	178056	42.8	5.0	68288	61.2	5.0	19752	26.6
5.0	93389	22.4	10.0	18316	16.4	10.0	25918	34.8
7.5	65820	15.8	15.0	12102	10.8	15.0	16197	21.8
10.0	33512	8.0	20.0	6575	5.90	20.0	7051	9.5
12.5	22556	5.4	25.0	3452	3.10	25.0	3127	4.2
15.0	6380	1.5	30.0	1185	1.06	30.0	1255	1.7
17.5	10246	2.5	35.0	881	0.79	35.0	571	0.77
20.0	1615	0.39	40.0	284	0.25	40.0	303	0.41
22.5	1586	0.38	45.0	122	0.11	45.0	60	0.08
25.0	640	0.15	50.0	120	0.11	50.0	26	0.03
27.5	856	0.20	55.0	24	0.02	55.0	27	0.03
30.0	280	0.07	60.0	25	0.02	60.0	30	0.04
32.5	375	0.09	65.0	27	0.02	65.0	42	0.06
35.0	55	0.02	70.0	33	0.03	70.0	16	0.02
37.5	512	0.12	75.0	56	0.05	75.0	26	0.03
N_v = 415877			N_v = 111488			N_v = 74000		

blends. From the above findings one can infer that, in the absence of adhesion or chemical reaction between matrix and dispersed phase, smaller rubbery particles seem to be more effective in generating high local stress concentrations.

Typical scanning electron micrographs of microtomed surfaces of B_2 and B_3 blends are reported in Fig. 4. Particle-size distribution curves are shown in Fig. 5. Looking at the curves and comparing with the data listed in Table IV, it emerges that in B_3 blend a finer dispersion of the EPR copolymer is achieved. The range of the EPR particles which results in such a blend is, in fact, about three times as narrow as that observed in B_2 blend. In B_3 blend most of the EPR particles have a diameter ranging from 2.5 and 20 μm and the largest particles measure 37.5 μm. On the other hand, in B_2 blend, most of the EPR particles exhibit a diameter ranging from 8.4 and 50 μm and the largest particles measure 125 μm. Consequently N_v for B_2 blend is found to be lower than that calculated for B_3 blend.

By comparing the particle size and the particle-size distribution of the blends, prepared during the hydrolitic polymerization of the CL (A_2 and B_2 blends) it is found that on increasing the EPR content a decrease in the value of N_v is observed (N_v = 111488 for A_2 and 40452 for B_2). Moreover in the case of A_2 blends, a large number of small particles (2.5 μm) are present.

As far as the blends prepared by melt mixing are concerned (A_3 and B_3 blends) both a decrease in EPR particle size and narrower particle size distribution, enhancing the EPR percentage are observed (compare Figs. 3 and 5, Tables III and IV). From the above it may be concluded that in 20% EPR containing blends, melt mixing seems to be more suitable in dispersing EPR. Such a finding may be accounted for by considering that in the case of preparation of blends concurrently with the hydrolytic polymerization of CL, the stirring of the system becomes less effective thus increasing the EPR content. The volumetric fraction values, estimated from the particle-size distribution are for B_2 and B_3 blends 24% and 27%, respectively. Such values are lower than calculated by composition and density of components (32.9%). Such a discrepancy is account for by the fact that some large EPR agglomerate was not taken into account.

4.2. Particle-size distribution in PA6/EPR/EPR-g-SA ternary blends

Typical scanning electron micrographs of microtomed surfaces of C_1 and C_2 blends are shown in Fig. 6. As shown by the data listed in Table V, a different

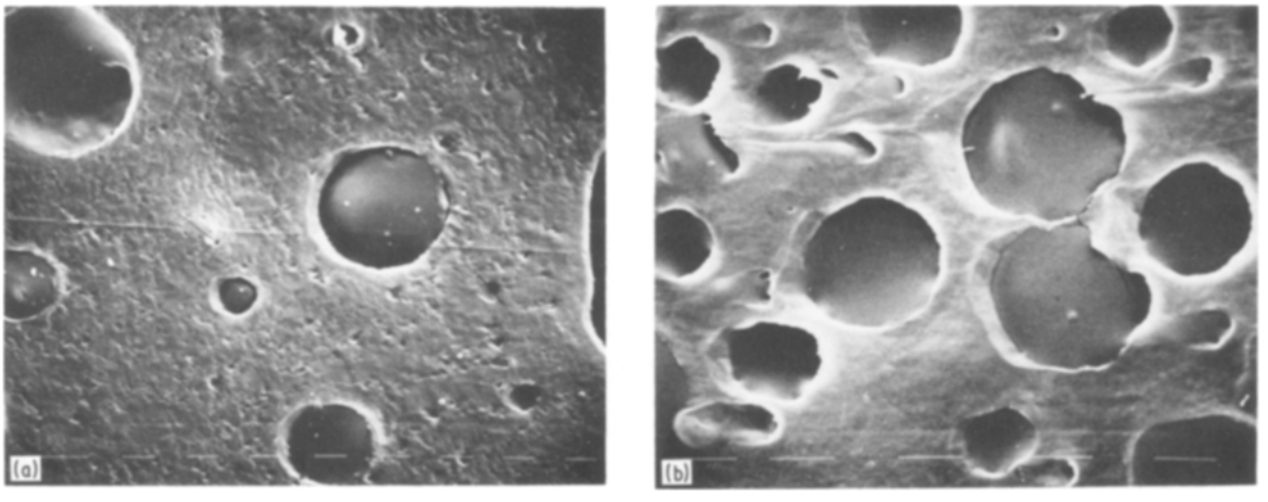

Figure 4 Scanning electron micrographs of microtomed surfaces of: (a) B_2 blend (×448); (b) B_3 blend (×875). PA6/EPR (80/20).

TABLE IV Particle diameters (D), number and per cent particles per volume unit (n_v and n_v %) of B_2 and B_3 blends. N_v is the total number of particles per volume unit

B_2			B_3		
D (μm)	n_v	n_v (%)	D (μm)	n_v	n_v (%)
8.4	35468	87.7	2.5	249744	43.6
16.7	1568	3.9	5.0	113270	19.8
25.1	994	2.4	7.5	75126	13.1
33.4	427	1.0	10.0	57974	10.1
41.8	959	2.4	12.5	36380	6.3
50.1	448	1.1	15.0	14087	2.5
58.4	154	0.38	17.5	8788	1.5
66.8	112	0.28	20.0	8337	1.4
75.2	183	0.45	22.5	3154	0.55
83.5	54	0.13	25.0	1944	0.34
91.8	16	0.04	27.5	155	0.03
100.2	18	0.45	30.0	1181	0.21
108.6	24	0.06	32.5	455	0.08
116.9	10	0.02	35.0	1210	0.21
125.2	15	0.04	37.5	319	0.06
N_v = 40452			N_v = 572128		

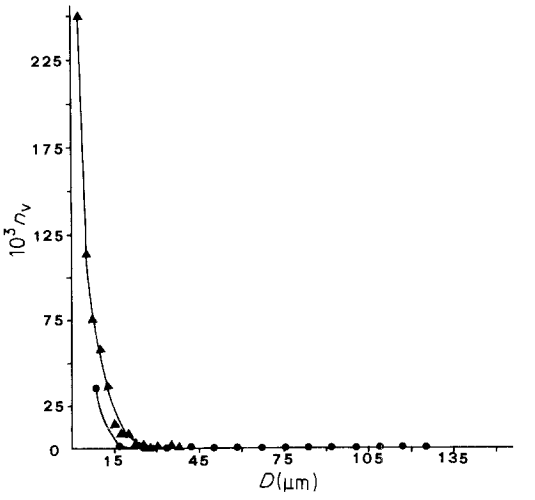

Figure 5 Particle-size distribution curves of (●) B_2 and (▲) B_3 blends.

particle-size distribution is found in C_1 and C_2 blends. In the case of C_1 the number of total particles per unit volume (N_v) is much higher than in C_2 (N_v = 1608636 for C_1 and only 24077 for C_2). Moreover a large number of dispersed particles with very small dimensions (D = 2.5 and 5 μm) is observed in C_1 samples. Finally, in C_1 blend the range of the size of rubbery particles is seen to be about four times narrower than that of C_2 (2.5 to 37.5 μm for C_1 and 10 to 150 μm for C_2). Thus it may be concluded that C_1 samples are characterized by a finer state of dispersion of the rubber component than that observed in the case of C_2 blend, and by a narrower particle-size distribution.

From the above results it appears that the dispersion of the rubbery components in xylene before the polymerization reaction starts is an essential step in order to realize a mixture where the functionalized EPR may act as emulsifier and compatibilizing agent. Contrary to expectations, the addition of functionalized EPR does not yield in C_2 blend a higher degree of dispersion of the rubbery phase than that observed in the binary PA6/EPR B_2 blend prepared according to the same procedure (compare Tables V and IV). In fact it can be seen that N_v is for B_2 blend higher than for C_2 (N_v = 40452 for B_2 and 24077 for C_2). Furthermore, particles with smaller dimensions are found in large amounts in the case of B_2 blend.

It is likely that the (EPR-g-SA)-g-PA6 graft copolymer, formed during the polymerization, cannot act efficiently as emulsifier. In fact the high reactivity of the anhydride groups probably leads to the formation of a graft copolymer, containing short PA6 branches. This graft copolymer tends to segregate giving rise to the formation of its own phase.

It is interesting to observe that C_2 blends show a better Izod impact behaviour than that of C_1 blend [4]. Such a result indicates that the mode and state of dispersion of the minor component observed for C_2 blend is more suitable in improving toughness than that of C_1 blend, even though in these latter blends a certain degree of adhesion between particle and matrix is observed, on etching the C_1 smoothed surface with boiling xylene vapours (see Fig. 7).

Particle-size distribution curves of D_1 and D_2 blends are shown in Figs. 8 and 9, respectively. It was observed in the case of the blends containing only the 2% functionalized EPR (C_1 and C_2 blend) that a finer

TABLE V Particle diameters (D), number and per cent particles per volume unit (n_v and n_v %) of C_1, C_2, D_1 and D_2 blends. N_v is the total number of particles per volume unit

C_1			C_2			D_1			D_2		
D (μm)	n_v	n_v (%)	D (μm)	n_v	n_v (%)	D (μm)	n_v	n_v (%)	D (μm)	n_v	n_v (%)
2.5	1276150	79.3	10.0	16866	70.1	0.8	7786653	51.5	5.0	28973	50.6
5.0	177248	11.0	20.0	5250	21.8	1.6	3748684	24.8	10.0	16886	29.5
7.5	60023	3.73	30.0	1019	4.23	2.5	1673806	11.1	15.0	5853	10.2
10.0	49830	3.10	40.0	387	1.61	3.3	806393	5.33	20.0	2920	5.1
12.5	18058	1.12	50.0	201	0.84	4.2	548499	3.63	25.0	971	1.70
15.0	11472	0.71	60.0	103	0.43	5.0	213067	1.41	30.0	653	1.14
17.5	5749	0.36	70.0	61	0.25	5.8	81599	0.54	35.0	653	1.11
20.0	3149	0.20	80.0	47	0.19	6.6	87240	0.58	40.0	221	0.39
22.5	2195	0.14	90.0	39	0.16	7.5	68730	0.45	45.0	47	0.08
25.0	1900	0.12	100.0	53	0.22	8.3	41266	0.27	50.0	12	0.02
27.5	938	0.06	110.0	25	0.10	9.2	17525	0.12	55.0	12	0.02
30.0	612	0.04	120.0	8	0.03	10.0	13464	0.09	60.0	12	0.02
32.5	514	0.03	130.0	4	0.02	10.8	18048	0.12	65.0	13	0.02
35.0	426	0.03	140.0	5	0.02	11.7	10.791	0.07	70.0	17	0.03
37.5	371	0.02	150.0	7	0.03	12.5	9376	0.06	75.0	26	0.05
N_v = 1608636			N_v = 24077			N_v = 15125144			N_v = 57252		

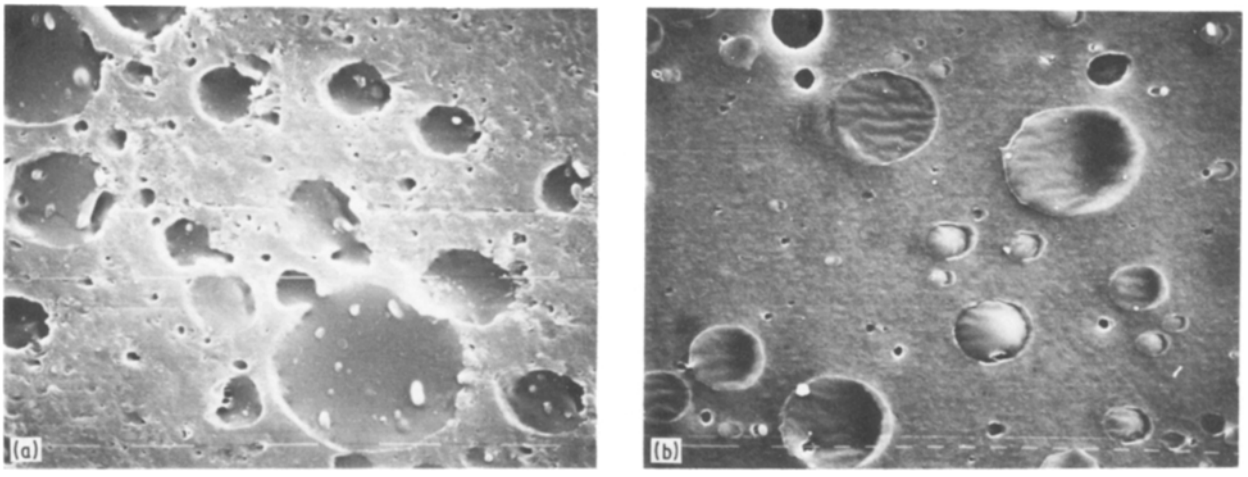

Figure 6 Scanning electron micrographs of microtomed surfaces of: (a) C_1 blend (× 875); C_2 blend (× 224). PA6/EPR/EPR-g-SA (80/18/2).

dispersion of the rubbery phase is exhibited by the blend obtained following the solution procedure (D_1 blend). As shown in Fig. 8 and Table V, in such a blend most of the particles have a diameter ranging from 1 to 5 μm, whereas in D_2 blend it ranges from 5 to 35 μm. The remarkable higher dispersion degree of the minor components, achieved in D_1 blend, also stands out when comparing N_v values of D_1 and D_2 blends. In D_1 blend there are about 15 000 000 particles per mm^3; on the other hand, there are only 57 000 particles per mm^3 counted in D_2 blend.

By comparing the particle-size distribution curve of C_2 and D_2 and of C_1 and D_1 (see Figs 8 and 9) it emerges that the addition of a larger amount of EPR-g-SA (5%) gives rise to a higher dispersion degree of the rubbery phase in the PA6, irrespective of the procedure used. It is, moreover, interesting to observe that a more remarkable improvement in dispersion degree of the minor components results in the blends obtained according to the solution preparative method. This finding suggests that the molecular structure and the amount of (EPR-g-SA)-g-PA6 copolymer, formed during blending, and its capability to act as emulsifier agent, may depend on the mixing conditions. It is likely that the dispersion of the rubbery components in xylene give rise to the formation of a rubber–rubber mixture where the functionalized EPR is finely dispersed. Consequently, during polymerization the EPR-g-SA molecules have more chance to come into contact with growing PA6 chains.

In the case of D_3 blend, the range of particle diameters is wider than that observed in D_1 but narrower than that of D_2 blend (see Tables V and VI). In D_3 blend most of the particles have diameters lying between 1.25 and 8.75 μm.

It is to be noted that for the B_3 binary blend, obtained by the same blending method, a higher degree of dispersion of the rubbery phase is achieved (about 5 000 000 particles per 1 mm^3 blend, whereas there are only 570 000 particles per mm^3 B_3 blend). Such a result indicates that the (EPR-g-SA)-g-PA6 copolymer formed during blending has the capability to act as emulsifier agent, so promoting finer dispersion of the minor components in the PA6.

As far as impact strength is concerned, it appears that, irrespective of the preparation method, D_1 and D_2 blends show the same impact behaviour. Moreover the Izod impact properties of such blends are slightly better than those of D_3 blend obtained by melt mixing [4].

Comparing particle sizes of D_3 blend with the particle size of E_3 blend, containing 10% functionalized EPR, it can be seen that the addition of a greater amount of EPR-g-SA copolymer does not change the range of particle diameters but affects the particle-size distribution. As shown in Fig. 10 the particle-size

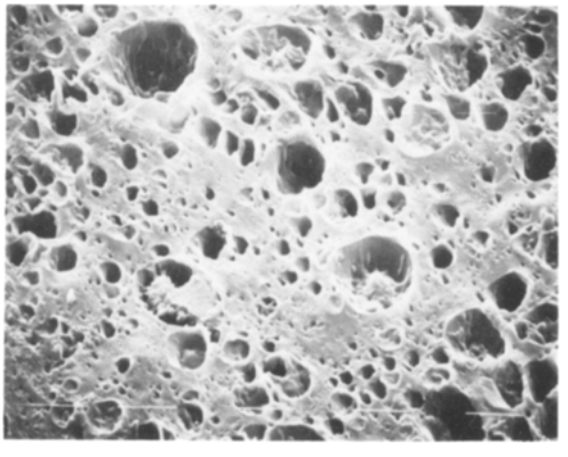

Figure 7 Scanning electron micrographs of C_1 smoothed surfaces etched with boiling xylene vapours (× 810). PA6/EPR/EPR-g-SA (80/18/2).

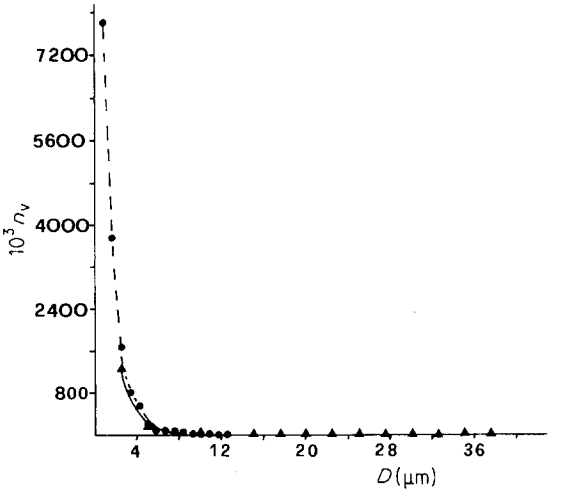

Figure 8 Particle-size distribution curves of (▲) C_1 and (●) D_1 blends.

TABLE VI Particle diameters (D), number and per cent particles per volume unit (n_v and n_v %) of D_3 and E_3 blends. N_v is the total number of particles per volume unit

D_3			E_3		
D (μm)	n_v	n_v (%)	D (μm)	n_v	n_v (%)
1.25	2200997	44.1	1.25	4386406	61.0
2.50	1456281	29.2	2.50	1531899	21.3
3.75	702189	14.1	3.75	534685	7.4
5.00	281299	5.6	5.00	246324	3.4
6.25	173894	3.5	6.25	206369	2.9
7.50	70296	1.4	7.50	111488	1.6
8.75	45279	0.91	8.75	45705	0.64
10.00	22630	0.45	10.00	55112	0.77
11.25	17209	0.34	11.25	16149	0.22
12.50	8819	0.18	12.50	4660	0.06
13.75	2188	0.04	13.75	12850	0.18
15.00	2526	0.05	15.00	7399	0.10
16.25	3462	0.07	16.25	8407	0.12
17.50	862	0.02	17.50	11407	0.16
18.75	1362	0.03	18.75	9930	0.14
N_v = 4989474			N_v = 7188796		

distribution of the rubbery phase in E_3 blend is characterized by a higher number of particles with small dimensions. Moreover, the E_3 N_v values are higher than those of D_3 N_v.

Finally it was found that the Izod impact properties of E_3 blend are better [5] than those observed in D_3 blend, suggesting that the particle-size distribution

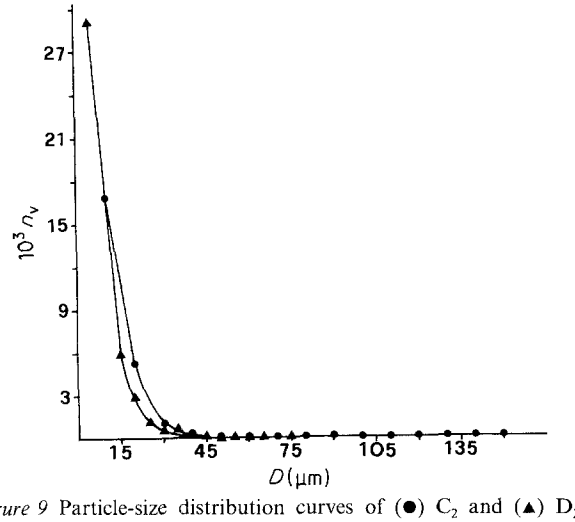

Figure 9 Particle-size distribution curves of (●) C_2 and (▲) D_2 blends.

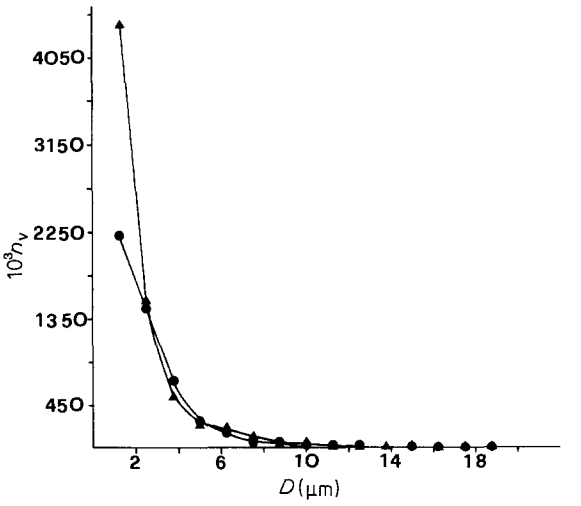

Figure 10 Particle-size distribution curves of (●) D_3 and (▲) E_3 blends.

achieved in E_3 blend is more suitable for inducing toughening characteristics to polyamide.

References

1. E. MARTUSCELLI, R. PALUMBO and M. KRYSZEWSKI, "Polymer Blends, Processing, Morphology and Properties" (Plenum, New York, 1980).
2. M. KRYSZEWSKI, E. MARTUSCELLI and R. PALUMBO, "Polymer Blends", Vol. 2 (Plenum, New York, 1984).
3. S. CIMMINO, L. D'ORAZIO, R. GRECO, G. MAGLIO, M. MALINCONICO, C. MANCARELLA, E. MARTUSCELLI, R. PALUMBO and G. RAGOSTA, *Polym. Engng Sci.* **24** (1984) 48.
4. S. CIMMINO, L. D'ORAZIO, R. GRECO, G. MAGLIO, M. MALINCONICO, C. MANCARELLA, E. MARTUSCELLI, P. MUSTO, R. PALUMBO and G. RAGOSTA, *ibid.* **25** (1985) 193.
5. S. CIMMINO, F. COPPOLA, L. D'ORAZIO, R. GRECO, G. MAGLIO, M. MALINCONICO, C. MANCARELLA, E. MARTUSCELLI and G. RAGOSTA, *Polymer* **27** (1986) 1874.
6. DE HOFF-RHINES. "Quantitative Microscopy" (McGraw-Hill, New York, 1986).

Received 11 February
and accepted 29 April 1987